01 Jan 2022

Monte Carlo Particle Simulation of Avalanche Breakdown in a Reverse Biased Diode with Full Band Structure

Zeyi Sun
Missouri University of Science and Technology, sunze@mst.edu

Manish Kizhakkeveettil Mathew

Ryan From

DongHyun Kim
Missouri University of Science and Technology, dkim@mst.edu

Recommended Citation

Z. Sun et al., "Monte Carlo Particle Simulation of Avalanche Breakdown in a Reverse Biased Diode with Full Band Structure," *Proceedings - Electronic Components and Technology Conference*, pp. 2287 - 2291, Institute of Electrical and Electronics Engineers, Jan 2022.
The definitive version is available at https://doi.org/10.1109/ECTC51906.2022.00361

2022 IEEE 72nd Electronic Components and Technology Conference (ECTC) | 978-1-6654-7943-1/22/$31.00 ©2022 IEEE | DOI: 10.1109/ECTC51906.2022.00361

Monte Carlo Particle Simulation of Avalanche Breakdown in a Reverse Biased Diode with Full Band Structure

Ze Sun
EMC Laboratory
Missouri University of S&T
Rolla, USA
sunz1@umsystem.edu

Manish Kizhakkeveettil Mathew
EMC Laboratory
Missouri University of S&T
Rolla, USA
mkmbzm@mst.edu

Ryan From
System, Support and Analytics
Boeing Research & Technology
St. Louis, USA
ryan.from@boeing.com

DongHyun Kim
EMC Laboratory
Missouri University of S&T
Rolla, USA
dkim@mst.edu

***Abstract*—To model the avalanche breakdown of a voltage regulator diode under reverse bias, a computationally rigorous device physics model using the Monte Carlo method to solve charge carrier Boltzmann transport equations (BTEs) is proposed. The transport of energetic charge carriers is calculated by using the full energy band instead of the non-parabolic band structure. The position-dependent doping profile found in real diodes is modeled accurately and time-efficiently. A two-step method is introduced to accelerate the simulation of avalanche breakdown. With the proposed model, the expected IV characteristics of a voltage regulator diode under reverse bias are simulated. The transport of charge carriers and avalanche breakdown are modeled at the microscopic level, and the simulation results are verified through comparison with the IV characteristics from the datasheet. This model can be used to analyze device susceptibility to electrical stress, providing a graphical visualization for failure mechanisms.**

***Index Terms*—Voltage regulator diode, Monte Carlo particle simulation, avalanche breakdown**

I. Introduction

VOLTAGE regulator diodes are widely used to protect electronic devices from failures caused by electrical overstress (EOS) and electrostatic discharge (ESD) [1]. When the current and voltage applied to the IC under protection are exceed the maximum rating, the reversed biased diode breaks down and provides a low impedance path between the IC and the ground. When selecting suitable voltage regulator diodes for the IC, the current and voltage (IV) characteristics of diodes under reverse bias are critical because they provide information including the clamping voltage and the on-resistance of the diode.

Traditionally, circuit models were built to model the IV characteristics of diodes. However, accurate circuit-level simulation is available only after fabrication and measurement of the discrete component. Therefore, a model to predict accurate IV characteristics is necessary to forecast and optimize chip security from EOS or ESD in early design stage.

The Boltzmann transport equation (BTE) describes the statistical behavior of charge carriers in a state out of equilibrium [2] [3]. The Monte Carlo (MC) method provides a direct solution to the BTE [4] and thus is used herein to characterize the IV of a reversed biased diode. Herein, several techniques are proposed to modify the traditional MC algorithm to improve both the accuracy and speed of the simulation.

First, previous MC simulations have focused mainly on the simulation of devices under normal working conditions. In this situation, the energy of charge carriers is relatively low, and the energy band of semiconductors can be approximated by a parabolic or non-parabolic model [5]. When avalanche breakdown occurs, charge carriers become energetic and the full-band structure of the semiconductor is necessary to accurately describe the transport of energetic particles [6].

Furthermore, when demonstrating the strength of the MC simulation, previous studies have usually used devices with uniform doping as examples for simplicity [7]. In reality, owing to the limitations of manufacturing techniques, the doping profile of the device can never be uniform. Using the previous simplified algorithm to model position-dependent doping leads to an enormous number of particles under simulation, thus substantially slowing the simulation without providing any accuracy improvement. Herein, a new method is proposed to model the position-dependent doping profile in an accurate, time-efficient manner.

Third, in the previous MC simulation, the avalanche breakdown is modeled by injecting charge carriers on the boundary of the depletion layer and counting the number of ionization events as the particles travel through the high electric field region [8]. This method is time-consuming, because the number of particles under simulation increases exponentially when avalanche breakdown occurs. Herein, a two-step algorithm is introduced to accelerate the calculation. Beyond modeling the avalanche breakdown of the reversed diode, the proposed model can also be used to analyze device susceptibility to other electrical stresses and attacks, thus providing a graphical visualization for failure mechanisms.

This article is organized as follows. In section II, the basics of BTE are reviewed, and the implementation of the full energy band is introduced. In section III, a new method to handle the position-dependent doping profile of semiconductor devices is proposed. A two-step method is then demonstrated

2377-5726/22/$31.00 ©2022 IEEE
DOI 10.1109/ECTC51906.2022.00361

in section IV to simulate the avalanche breakdown and identify the clamping voltage of the voltage regulator diode. Section V concludes the article.

II. Boltzmann Transport Equation Solver

The BTE describes the change in the particle distribution function $f(t, \mathbf{x}, \mathbf{k})$ over time by considering both the energy and momentum conservation of particles, as shown in Eq. 1 [9]. Here, f describes the probability of finding a particle located at position $\mathbf{x}$ with wave vector $\mathbf{k}$ at time t. The left-hand side of the equation describes the collisionless advection, wherein the second term represents the diffusion of particles due to the gradients in carrier concentration or temperature, and the third term is associated with the electric and magnetic field effects. The right-hand side of the equation represents the effects of the collisions.

$$\frac{\partial f}{\partial t} + \mathbf{v} \cdot \nabla_{\mathbf{x}} f + \frac{\partial \mathbf{k}}{\partial t} \cdot \nabla_{\mathbf{k}} f = \left(\frac{\partial f}{\partial t}\right)_{coll} \tag{1}$$

The MC technique is used to solve the BTE. The transport of charge carriers is determined by free flights and scattering events. During the free flights, particles are driven by the external force due to electric and magnetic fields. The time between two successive collisions and the mechanism of scattering events are selected stochastically according to the pre-defined scattering rates [2].

To model the transport of energetic charge carriers when avalanche breakdown occurs, the full energy band, rather than the non-parabolic approximation, is used [10]. A mesh of $\mathbf{k}$ points in the $\frac{1}{48}$ irreducible wedge of the Brillouin zone is created. The distance between two adjacent $\mathbf{k}$ points is $0.02(\frac{2\pi}{a})$, where a is the lattice constant. The corresponding energy on these mesh points is calculated with the empirical local pseudo-potential method. The data for the first four conduction bands and the first three valence bands are considered. The density of states and the corresponding scattering rates are also calculated on these mesh points. The non-polar optical phonon scattering, acoustic phonon scattering, and impurity scattering are included.

The drift of charge carriers due to electric field (ignoring magnetic field effects) is governed by the equations of motion:

$$\frac{d\mathbf{k}}{dt} = \frac{q}{\hbar}\nabla_r \phi(\mathbf{x}) = -\frac{q\mathbf{F}(\mathbf{x})}{\hbar} \tag{2}$$

$$\frac{d\mathbf{x}}{dt} = \frac{1}{\hbar}\nabla_{\mathbf{k}} E(\mathbf{k}) \tag{3}$$

where $\phi(\mathbf{x})$ is the electric potential, q is the elementary charge, $\mathbf{F}$ is the electric field intensity, $\hbar$ is the reduced Planck constant, and $\mathbf{E}$ is the calculated energy band. During each free flight, change in $\mathbf{k}$ is first calculated. Next, the corresponding particle energy before and after the drift is obtained. $\nabla_{\mathbf{k}} E(\mathbf{k})$ in Eq. 3 is numerically approximated as the ratio between the energy change and the wave vector change during the free flight. In this way, the velocity of drift is calculated, and the positions of particles are updated.

After the free flight, the closest mesh point near the current wave vector $\mathbf{k}$ is found, and the corresponding scattering rate is loaded. As in the classical MC algorithm, a random number is generated to determine the scattering type. After the collision, the energy of the particle may change because of either phonon absorption or emission. After the final energy is known, all mesh points in the first brillouin zone (FBZ) with similar energy on a certain band are found first. They are then weighted by their density of states, and the final wave vector $\mathbf{k}$ after the scattering is randomly selected among them.

III. Position-Dependent Doping Profile

To illustrate the proposed algorithm, a real voltage regulator diode that can be found on the market is simulated as an example. The doping profile of the diode is shown in Fig. 1a. The exact value of geometrical size and doping density is not shown here due to confidential issues. Silicon is doped with bron and phosphorus from the top and antimony from the substrate. The doping density varies only with the position along the axis shown in the figure and does not change in the perpendicular plane. The net doping density can be obtained by subtracting the antimony and phosphorus density from the boron profile, as shown in Fig. 1b. The left part of the diode is P-doped, and the right part is N-doped.

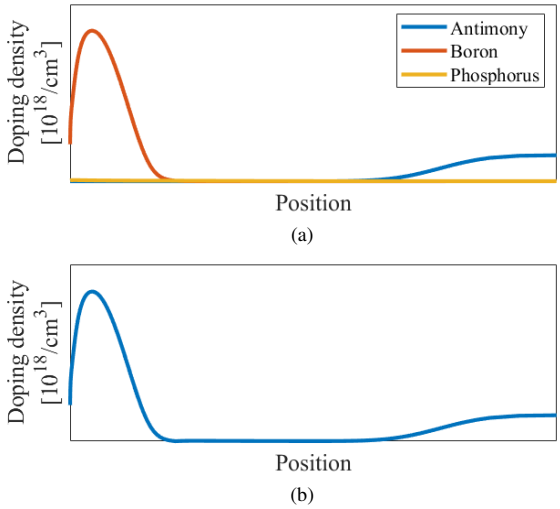

Fig. 1: (a): Doping profile of the diode under simulation. (b): Absolute value of the net doping density.

In the MC simulation, the change in the charge distribution function $f(t, \mathbf{x}, \mathbf{k})$ is obtained by following the motion of many particles. Each particle under simulation represents a certain amount of charge. This value is called the charge per super particle (*cpsp*) and is a constant in most previous studies. However, for the diode under simulation herein, the net doping density changes significantly at different positions. The position with the maximum doping density is located at the P-doped region, and the position with the minimum doping density is located at the boundary between P- and N-doped

region, as shown in Fig. 2. The ratio between the maximum and minimum doping density is approximately 30,000. If *cpsp* remains a constant, and one particle is initially placed at the minimum doping position, then 30,000 particles must correspondingly be placed at the maximum doping position. In this way, an enormous number of particles would be included in the simulation, thus significantly increasing the calculation time.

To avoid the large particle number without decreasing the simulation accuracy, the idea of position-dependent *cpsp* is introduced. The computational domain is divided into eight sections according to the net doping density, as shown in Fig. 2a. The boundary of each section is selected to ensure that the ratio between the maximum and minimum doping density of each section is less than 150.

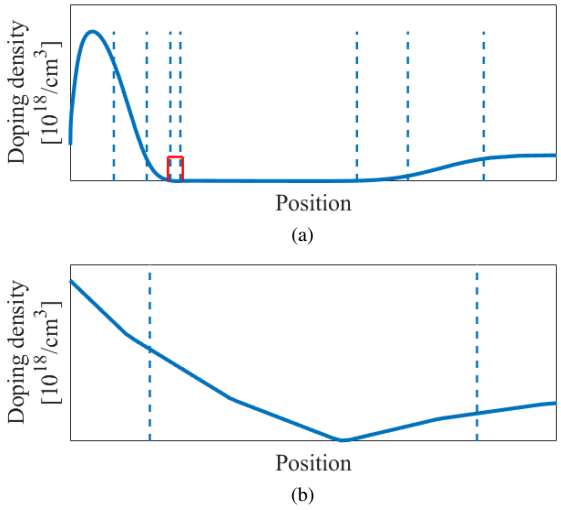

Fig. 2: (a): Division of the whole domain into eight sections. (b): Zoom view of the area in the red box in Fig. 2a where the doping density is lowest.

Next, within each section, the position with the lowest doping density is found. Five particles are initialized at these positions. Then the corresponding *cpsp* for each section is calculated with Eq. 4. On the boundary of two adjacent sections, the value of *cpsp* changes linearly rather than abruptly. Otherwise, when one particle with a relatively large *cpsp* drifts across the border, the charge distribution of the neighboring section significantly changes in a non-physical manner, thus leading to the wrong potential distribution. The final *cpsp* distribution at different locations is shown in Fig. 3. The number of particles that must be initialized at each mesh cell is shown in Fig. 4. With respect to the use of the same *cpsp* for the whole domain, the total number of particles decreases by 99%.

$$cpsp = \frac{minimum\ doping\ density \times triangle\ cell\ area}{5} \tag{4}$$

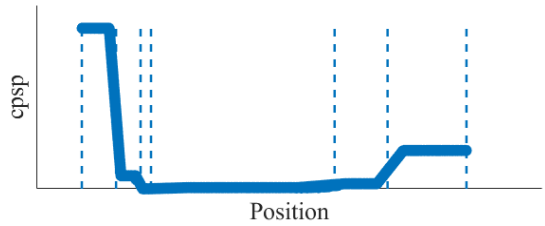

Fig. 3: Distribution of *cpsp* at different locations.

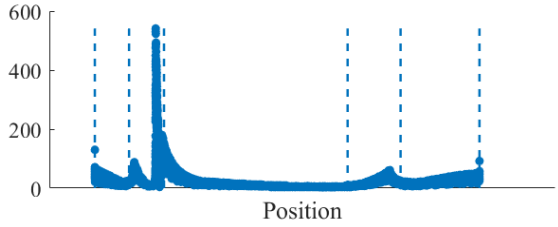

Fig. 4: Number of particles per cell when initialization.

IV. Avalanche Breakdown

After initialization of the particles, different reverse bias voltages are applied across the diode, and the corresponding electrostatic potential distribution is obtained through MC simulation, as shown in Fig. 5. A thin depletion layer is formed between the p-doped and n-doped area when the charge distribution stabilizes. The potential changes dramatically in the depletion layer, but remains flat in the p-doped and n-doped region.

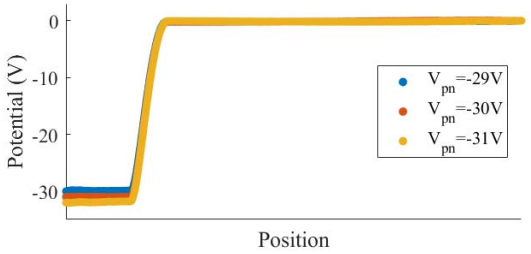

Fig. 5: Potential distribution across the diode under different reverse bias voltages.

Traditionally, to determine the threshold reverse bias voltage leading to avalanche breakdown, some electrons are injected on the edge of the depletion layer at the P-doped side (or some holes are injected on the edge of the depletion layer at the N-doped side). The potential distributions under different bias voltages are loaded and remain unchanged during the simulation. As the electrons (or holes) travel through the depletion layer, they are accelerated by the strong E-field. When their energy is sufficiently high, ionization may occur, and a new electron and hole pair will be generated. The original electron (or hole) and the newly generated electron-hole pair will continue to drift under the strong E-field and

may further lead to new ionization events. The simulation does not stop until all electrons and holes leave the depletion layer. The multiplication factor is defined as the ratio between the number of ionization events and the number of initially injected particles. The multiplication factor is expected to be small when the bias voltage is low but to dramatically increase when the bias voltage crosses a threshold. The turning point of the bias voltage versus multiplication factor curve is the clamping voltage of the voltage regulator diode.

The problem with the traditional method is that when the bias voltage is near to or higher than the clamping voltage, ionization introduces an enormous number of particles into the simulation, thus leading to a long simulation time. To accelerate the calculation, a two-step method is introduced herein.

In step #1, the electrostatic potential distribution obtained from the previous simulation is first loaded. Because the ionization occurs only in the region where the E-field is strong, when determining the clamping voltage of the diode, only the depletion layer is considered, as shown in Fig. 6.

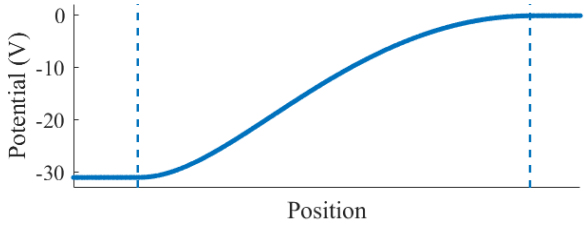

Fig. 6: Potential distribution in the depletion layer when the reverse bias voltage is $30V$. The two dashed lines indicate the edge of the depletion layer.

Next, the depletion layer is uniformly divided into 100 subsections. A total of 50 electrons are injected at the first subsection on the left most side. Ionization may occur as these electrons travel to the right edge of the depletion layer. In contrast to the traditional method, the transport of the new electron-hole pair is not included in the following calculation. Only the energy of the particle is decreased to maintain the energy and momentum conservation during the ionization. In this way, the number of particles under simulation does not increase. The position where the ionization occurs is recorded for future use. This simulation reveals when an electron is injected at the first subsection, the number of ionization events expected to occur as it travels through the depletion layer, and where these ionization events occur.

The same simulation is repeated for each subsection. In each simulation, 50 electrons are injected at different locations and travel through the depletion layer, and the number and position of ionization events are recorded. Furthermore, similar simulations are performed by injecting holes at each subsection and recording the ionization positions.

Step #2 uses the results in step #1 to predict when and where ionization will occur. First, 50 electrons are injected from the left edge of the depletion layer and are called the first generation. MC simulation is not performed at this point to calculate the transport of these electrons. Instead, from the results in step #1, the positions where the ionization will occur when electrons are injected at subsection #1 are already known. The newly generated electron-hole pairs are called the second generation, as shown in Fig. 7a.

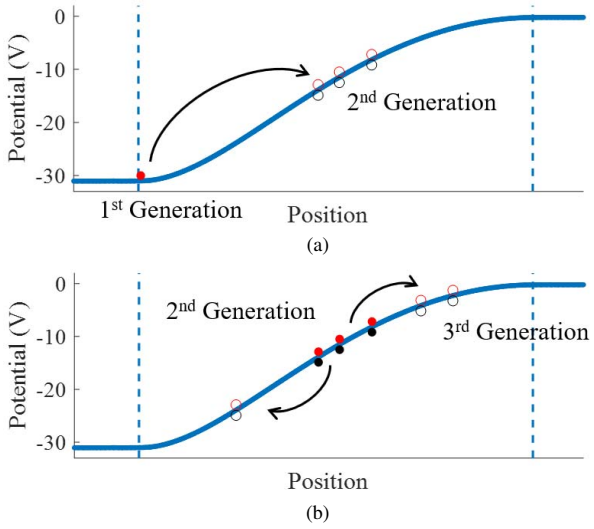

Fig. 7: (a): Expected ionization positions as the first generation electrons travel to the right. The second generation is created after the ionization. Newly generated electrons and holes are represented as red and black empty circles, respectively. (b): Second generation electrons drift to the right, whereas while holes drift to the left, both of which may cause ionization. The newly generated particles are called the third generation.

Subsequently, the subsection where each second generation particle is located is determined. The corresponding results of these subsections in step #1 are loaded. These results indicate where the ionization will occur when particles are injected at these locations and travel through the depletion layer. The newly generated electron-hole pairs are called the third generation, as shown in Fig. 7b.

According to the injection position of the third generation, the generation position of the fourth generation can be determined. This iteration does not stop until no new electron-hole pairs are generated. Fig. 8 shows the change in the normalized total number of ionization events over generations. When the bias voltage is low (less than 30 V in this case), the E-field strength in the depletion layer is relatively weak. After several generations, all particles leave the depletion layer, and no further ionization events occur. Thus, the curve quickly becomes flat. When the bias voltage is high (greater than 30 V in this case), the curve continues to rise for more than 1000 generations, which means a strong E-field leads to avalanche breakdown. Thus, the clamping voltage of this diode is $30V$, in agreement with the specifications in the datasheet. Furthermore, the IV curve from the datasheet is shown in Fig. 9. The current quickly increases as long as the reverse bias

voltage reaches $30V$, in good agreement with the simulation results.

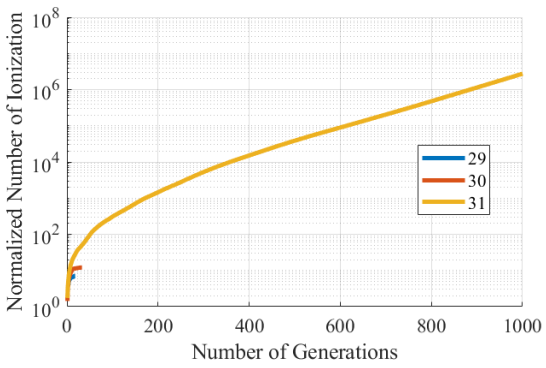

(a)

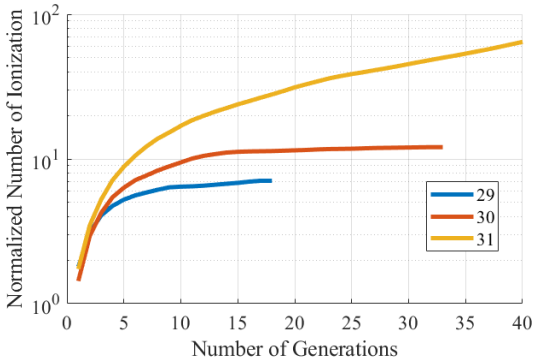

(b)

Fig. 8: (a): Change in the normalized total number of ionization events over generations; (b): Zoom view of the first 40 generations.

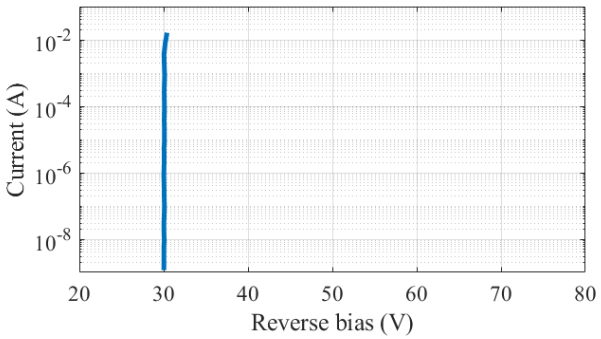

Fig. 9: IV curve from datasheet.

V. Conclusion

To simulate the avalanche breakdown of a voltage regulator diode under reverse bias, several features are introduced to enhance the traditional MC method. The full energy band is used to calculate the drift and scattering of energetic charge carriers. The position-dependent *cpsp* is introduced to model the doping profile of the diode in an accurate and time-efficient manner. A two-step method is used to avoid the exponential increase in particles under simulation in the avalanche breakdown. The simulation results enable understanding of charge transport at the microscopic level and can reveal device failure mechanisms under extreme working conditions. Guidelines and tools will be further developed to optimize the chip security from EOS or ESD in early design stages, and fixing existing weak spots in currently used integrated protection designs.

VI. Acknowledgment

This work was supported partly by the National Science Foundation under grant No. IIP-1916535.

References

[1] Marathe, S., Wei, P., Ze, S., Guan, L. and Pommerenke, D., 2017, September. Scenarios of ESD discharges to USB connectors. In 2017 39th Electrical Overstress/Electrostatic Discharge Symposium (EOS/ESD) (pp. 1-6). IEEE.

[2] Hockney, R.W. and Eastwood, J.W., 2021. Computer simulation using particles. crc Press.

[3] Moglestue, C., 2013. Monte Carlo simulation of semiconductor devices. Springer Science & Business Media.

[4] Sun, Z., Erickson, N., Sun, J., From, R. and Fan, J., 2019, May. Monte Carlo Particle Simulation for Electrical and Thermal Analysis of a MESFET using the Finite-Element Approach. In 2019 IEEE MTT-S International Conference on Numerical Electromagnetic and Multiphysics Modeling and Optimization (NEMO) (pp. 1-4). IEEE.

[5] Awano, Y., Tomizawa, K., Hashizume, N. and Kawashima, M., 1983. Monte Carlo particle simulation of a GaAs short-channel MESFET. Electronics Letters, 19(1), pp.20-21.

[6] Kunikiyo, T., Takenaka, M., Kamakura, Y., Yamaji, M., Mizuno, H., Morifuji, M., Taniguchi, K. and Hamaguchi, C., 1994. A Monte Carlo simulation of anisotropic electron transport in silicon including full band structure and anisotropic impact-ionization model. Journal of Applied Physics, 75(1), pp.297-312.

[7] Zhang, Z., Zhang, L., Sun, Z., Erickson, N., From, R. and Fan, J., 2019, June. Solving Poisson's Equation using Deep Learning in Particle Simulation of PN Junction. In 2019 Joint International Symposium on Electromagnetic Compatibility, Sapporo and Asia-Pacific International Symposium on Electromagnetic Compatibility (EMC Sapporo/APEMC) (pp. 305-308). IEEE.

[8] Zhou, X., Ng, J.S. and Tan, C.H., 2012. A simple Monte Carlo model for prediction of avalanche multiplication process in Silicon. Journal of Instrumentation, 7(08), p.P08006.

[9] Zhang, L., Huang, W., Sun, Z., Erickson, N., From, R. and Fan, J., 2020, July. Deep Learning Based Poisson Solver in Particle Simulation of PN Junction with Transient ESD Excitation. In 2020 IEEE International Symposium on Electromagnetic Compatibility & Signal/Power Integrity (EMCSI) (pp. 241-244). IEEE.

[10] Jallepalli, S., Rashed, M., Shih, W.K., Maziar, C.M. and Tasch Jr, A.F., 1997. A full-band Monte Carlo model for hole transport in silicon. Journal of applied physics, 81(5), pp.2250-2255.